Supporting Information for

Hierarchically Structured MIL-100(Al) Beads for Diffusion-Optimized Amine Sorbents in Direct Air Capture

Phat Ngoc Nguyen[a], Thach N. Tu*[,a], Hae-Kwon Jeong*[,a,b], and Jinsoo Kim*[,a]

[a] Department of Chemical Engineering (Integrated Engineering), Kyung Hee University, 1732 Deogyeong-daero, Giheung-gu, Yongin-si, Gyeonggi-do 17104, Republic of Korea.

[b] Artie McFerrin Department of Chemical Engineering, Texas A&M University, 3122 TAMU, College Station, TX 77843-3122, USA

Email: tungocthach1987@gmail.com, hjeong7@tamu.edu, jkim21@khu.ac.kr

Section S1: Materials, Analytical Techniques and Experimental Methods

Materials

Aluminum-tri-sec-butoxide (ALTSB, 97%), and poly(vinyl alcohol) (PVA, Mw 31,000-50,000, 98-99% hydrolyzed), Trimesic acid (95%), Ethylenediamine (EDA, 99%), Triethylamine (TEA, 99%), Diethylenetriamine (DETA, ReagentPlus®, 99%), Pentaethylenehexamine (PEHA, technical grade), N, N'-dimethylethylenediamine (MMEN, 98%), Toluene (anhydrous), Methanol (MeOH, 99.9%) were purchased from Sigma-Aldrich Nitric acid (HNO_3, 60%) was obtained from Daejung Chemical, Korea, and carbon nanotubes were purchased from Carbon Nano-material Technology Co.,Ltd, Korea. The purified water (18.2 MΩ·cm) was produced by an Aquapuri 541 (Youngin Chromass, Korea). All the chemicals were used without further purification.

Preparation of macroporous γ-alumina (Mac_γ-Al) beads: Boehmite sol (1M) was prepared by adding 0.1 mol ALTSB in the flask containing 100 mL of hot water (70-90°C) followed by stirring 1-2 hours continuously. Then, 7 mL 1M HNO_3 was slowly poured into the as-stirred Boehmite liquid, and the mixture was refluxed at 90-100°C for 10 hours. Carbon nanotubes (CNTs, multi-wall, 20 nm, 100 mg) were dispersed in a boehmite sol (1M, 4 mL) and homogenized by sonication and stirring, followed by the addition of a PVA solution (50g L^{-1}, 4 mL). The resulting suspension was stirred for 30 min and dropped into liquid N_2 to form frozen beads, which were subsequently solvent-exchanged in cold EtOH (-10 °C) to facilitate gradual water removal. After warming to room temperature, the beads were collected, vacuum-dried (1 h), and further dried at 70 °C overnight. Calcination at 650 °C in air for 12 h removed the CNT and PVA templates, yielding macroporous γ-Al_2O_3 beads.[1].

Analytical Techniques

Powder X-ray diffraction (PXRD) patterns were collected using a RIGAKU MiniFlex600 diffractometer. The morphology of the beads and the powder was determined by scanning

electron microscopy (SEM; Leo-Supra 55, Carl Zeiss STM). The CO_2, and N_2 isotherms at room temperature were collected using the BELSORP-mini with an equilibrium criterion of an adsorption amount change within 0.1 cm^3 g^{-1} over 300 s at each pressure step. Thermal gravimetric analysis (TGA) was performed under a gas mixture of O_2 (20%) and N_2 (80%) at a temperature ramp rate of 5 °C min^{-1}. Fourier transform infrared (FT-IR) spectra were measured on a PerkinElmer FT-IR spectrometer (Frontier model) using the ATR protocol. N_2 adsorption-desorption isotherms were measured at 77 K using a BELSORP-max instrument. Prior to the measurements, all as-synthesized samples were degassed at 150 °C under vacuum overnight to remove guest molecules and adsorbed moisture. The BET surface areas were calculated from the adsorption branch using the Brunauer-Emmett-Teller equation below. The fitting ranges were selected from the linear region of the BET plots and checked according to the BET consistency criteria.

BET equation:

$$\frac{1}{q\left(\frac{P_0}{P}-1\right)} = \frac{C-1}{q_m C}\left(\frac{P}{P_0}\right) + \frac{1}{q_m C} \qquad \text{(eq. 1)}$$

where q is the adsorbed amount at relative pressure P/P_0 , q_m is the monolayer capacity, and C is the BET constant. The BET surface area was calculated from:

$$S_{BET} = \frac{q_m N_A \sigma_{N_2}}{V_m} \qquad \text{(eq. 2)}$$

where σ_{N_2} is the molecular cross-sectional area of N_2, 0.162 nm^2, and V_m is the molar volume used for the adsorption units.

Calculation of amine loading within Mac_MIL-100Al beads

Amine mass fraction (wt%) from EA measurement:

$$w_{amine}\,(\%) = \frac{\Delta N}{f_{N,\ amine}} \qquad \text{(eq. 3)}$$

where

$$\Delta N = N_{func} - N_{pristine} \qquad \text{(eq. 4)}$$

is the increase in nitrogen content (wt% from EA), and

$$f_{N,\ amine} = \frac{n_N M_N}{M_{amine}} \qquad \text{(eq. 5)}$$

is the mass fraction of nitrogen in the amine (n_N = number of N atoms per amine molecules, M_N = 14.01 g mol^{-1}, M_{amine} = molar mass of the amine).

Molar amine loading (mmol g^{-1}):

$$n_{amine}\,(mmol\ g^{-1}) = \frac{w_{amine}/100}{M_{amine}} \times 1000 \qquad \text{(eq. 6)}$$

Moles of Al and Al_3 clusters per gram (from wt% Al)

$$n_{Al}\,(mmol\ g^{-1}) = \frac{w_{Al}/100}{M_{Al}} \times 1000 \qquad \text{(eq. 7)}$$

and

$$n_{Al_3}\,(mmol\ g^{-1}) = \frac{n_{Al}}{3} \qquad \text{(eq. 8)}$$

where w_{Al} is the wt% Al in the samples (calculated from TGA) and M_{Al} = 26.98 g mol^{-1}

Amine molecules per Al_3 cluster:

$$DETA\ per\ Al_3 = \frac{n_{amine}}{n_{Al_3}} \qquad \text{(eq. 9)}$$

Isosteric heat of CO_2 adsorption calculation

The isosteric heat of CO_2 adsorption (Q_{st}) was calculated from CO_2 adsorption isotherms measured at 298 and 318 K using the virial fitting method. The adsorption branch was used for fitting. The virial equation was expressed as:

$$lnP = lnq + \frac{1}{T}\sum_{i=0}^{m} a_i q^i + \sum_{j=0}^{n} b_j q^j \quad \text{(eq. 10)}$$

where P is the equilibrium pressure, q is the adsorbed amount, T is the absolute temperature, and a_i and b_j are virial fitting parameters. The isosteric heat of adsorption was calculated according to:

$$Q_{st} = -R\sum_{i=0}^{m} a_i q^i \quad \text{(eq. 11)}$$

where R is the gas constant. The virial fitting curves for DETA@Mac_MIL-100Al beads and the resulting Q_{st} profile are shown in Fig. S12.

Calculation of IAST selectivity:

Binary gas composition and partial pressures:

$$y_{CO_2} = 4.0 \times 10^{-4}, \quad y_{N_2} = 1 - y_{CO_2} = 0.9996$$

Partial pressures:

$$P_i = y_i P_{tot} \quad \text{(eq. 12)}$$

Pure-component isotherms and Henry's law:

$$q_i(P) \approx K_{H,i} P \quad \text{(eq. 13)}$$

where $K_{H,i}$ is the Henry constant.

$$K_H = \frac{\sum_k P_k q_k}{\sum_k P_k^2} \quad \text{(eq. 14)}$$

Spreading pressure:

The spreading pressure of pure component *i* is defined as

$$\pi_i(P) = \int_0^P \frac{q_i(p)}{p} dp \quad \text{(eq. 15)}$$

In IAST equilibrium, all components share a common spreading pressure π, and the corresponding equivalent pure-component pressure P^*_i satisfies

$$\pi = \pi_i(P^*_i) \quad \text{(eq. 16)}$$

IAST equilibrium condition and adsorbed-phase composition

The common spreading pressure π is obtained by solving

$$\sum_i \frac{P_i}{P^*_i(\pi)} = 1 \quad \text{(eq. 17)}$$

where $P^*_i(\pi)$ denotes the inverse mapping of Eq. 12. Once π is determined, the adsorbed-phase mole fractions x_i are given by

$$x_i = \frac{P_i}{P^*_i(\pi)}, \quad \sum_i x_i = 1 \quad \text{(eq. 18)}$$

CO_2/N_2 selectivity

The IAST selectivity of CO_2 over N_2 is defined as:

$$S_{CO_2/N_2} = \frac{x_{CO_2}/x_{N_2}}{y_{CO_2}/y_{N_2}} \quad \text{(eq. 19)}$$

Section S2. Characterization of Mac_MIL-100Al beads, DETA@Mac_MIL-100Al beads, MIL-100Al powder and DETA@MIL-100Al powder

Table S1. Elemental analysis

Element	Mac_MIL-100Al beads	DETA@Mac_MIL-100Al beads	DETA@Mac_MIL-100Al beads (after 5 cycles)	MIL-100Al powder	DETA@MIL-100Al powder
C	39.5	42.9	42.8	38.95	41.20
H	2.62	5.01	5.91	5.29	4.00
N	0.34	10.7	10.4	0.79	8.04

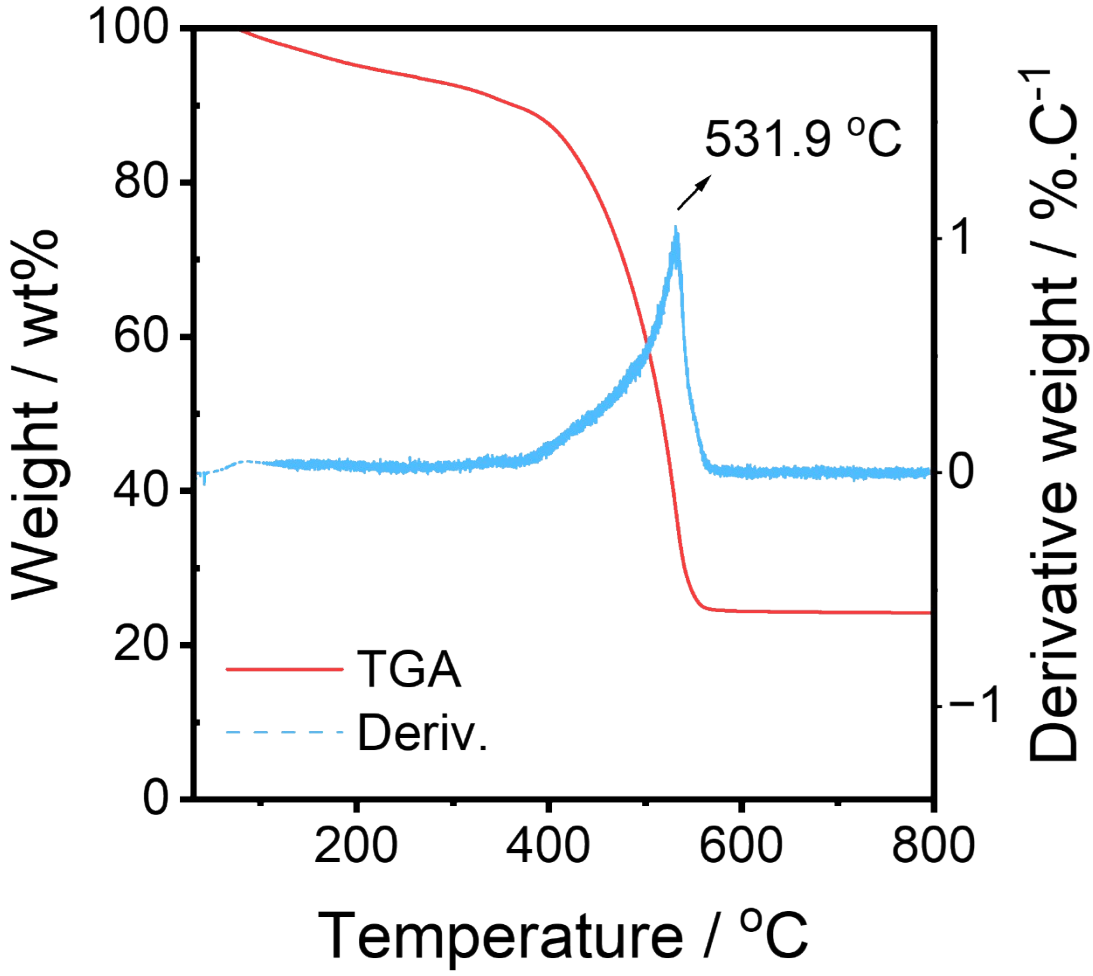

Figure S1. TGA profile of the Mac_MIL-100Al beads synthesized for 3 h.

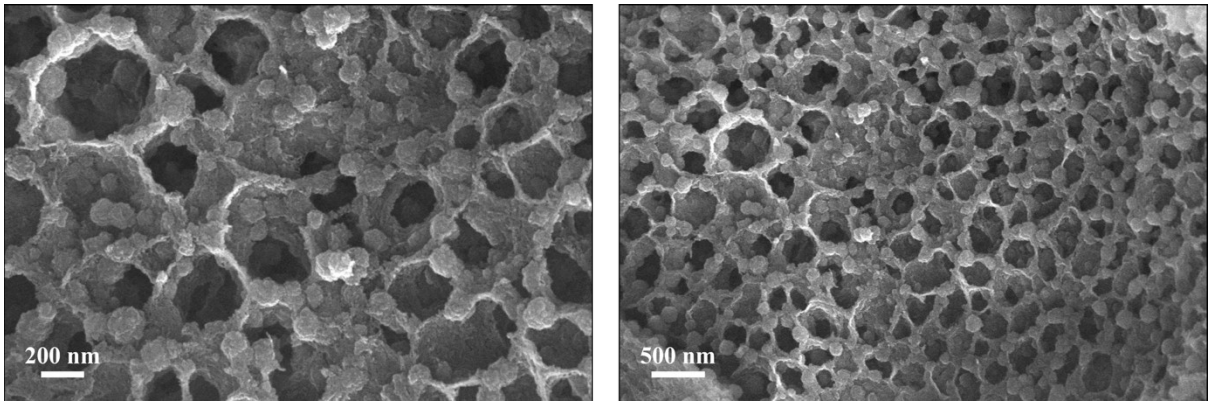

Figure S2. SEM images of 1-hour Mac_MIL-100Al beads.

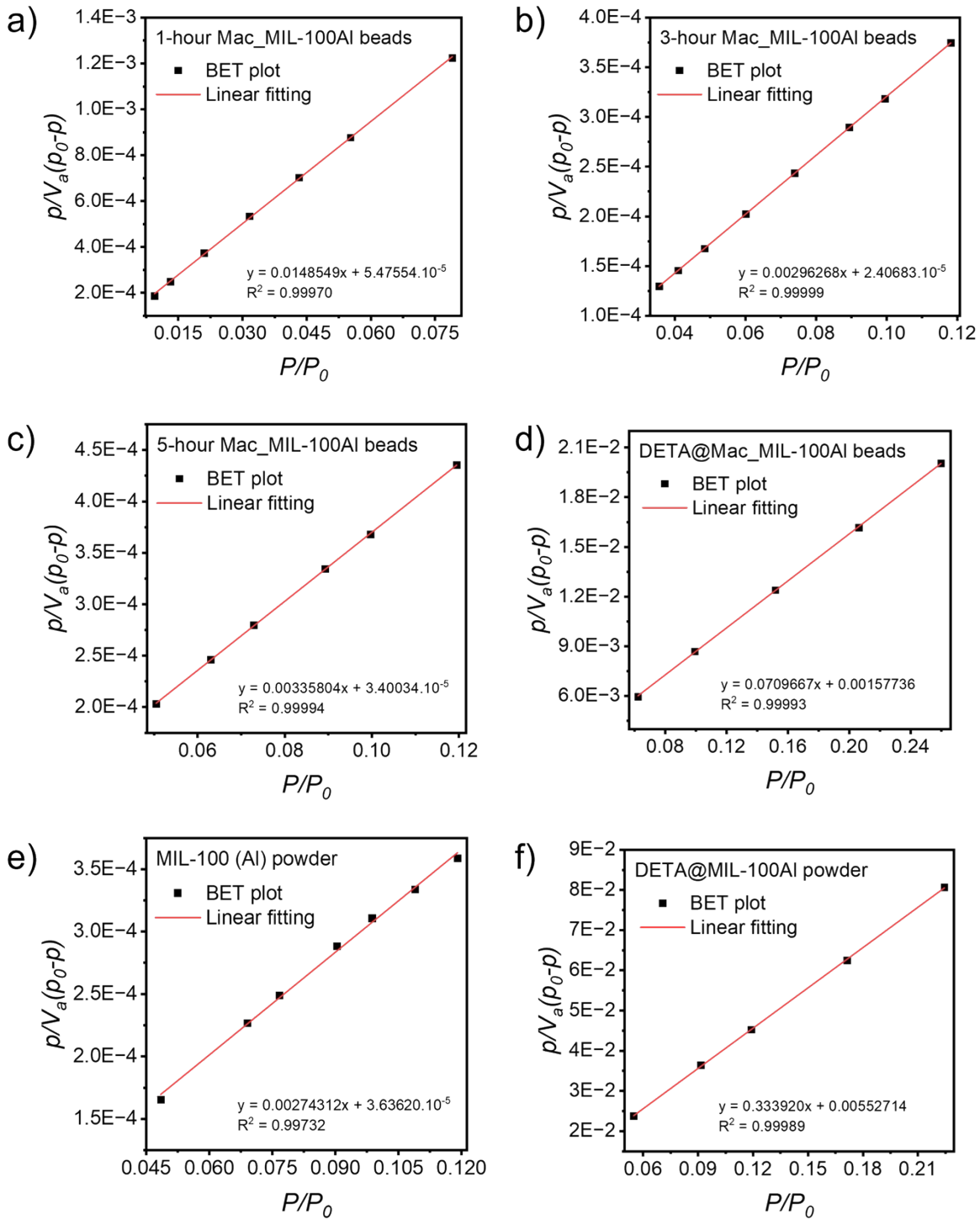

Figure S3. BET plots of (a) 1 h Mac_MIL-100Al beads, (b) 3 h Mac_MIL-100Al beads, (c) 5 h Mac_MIL-100Al beads, (d) MIL-100Al powder, and (e) DETA@Mac_MIL-100Al beads. The red lines indicate the linear fitting regions used for BET surface area calculation.

Table S2. Mechanical stability of Mac_MIL-100 beads

Sample size / mm^2	Stress at Break /MPa	Strain at Break / %	Young Modulus
7.5	0.1	34.28	3.28

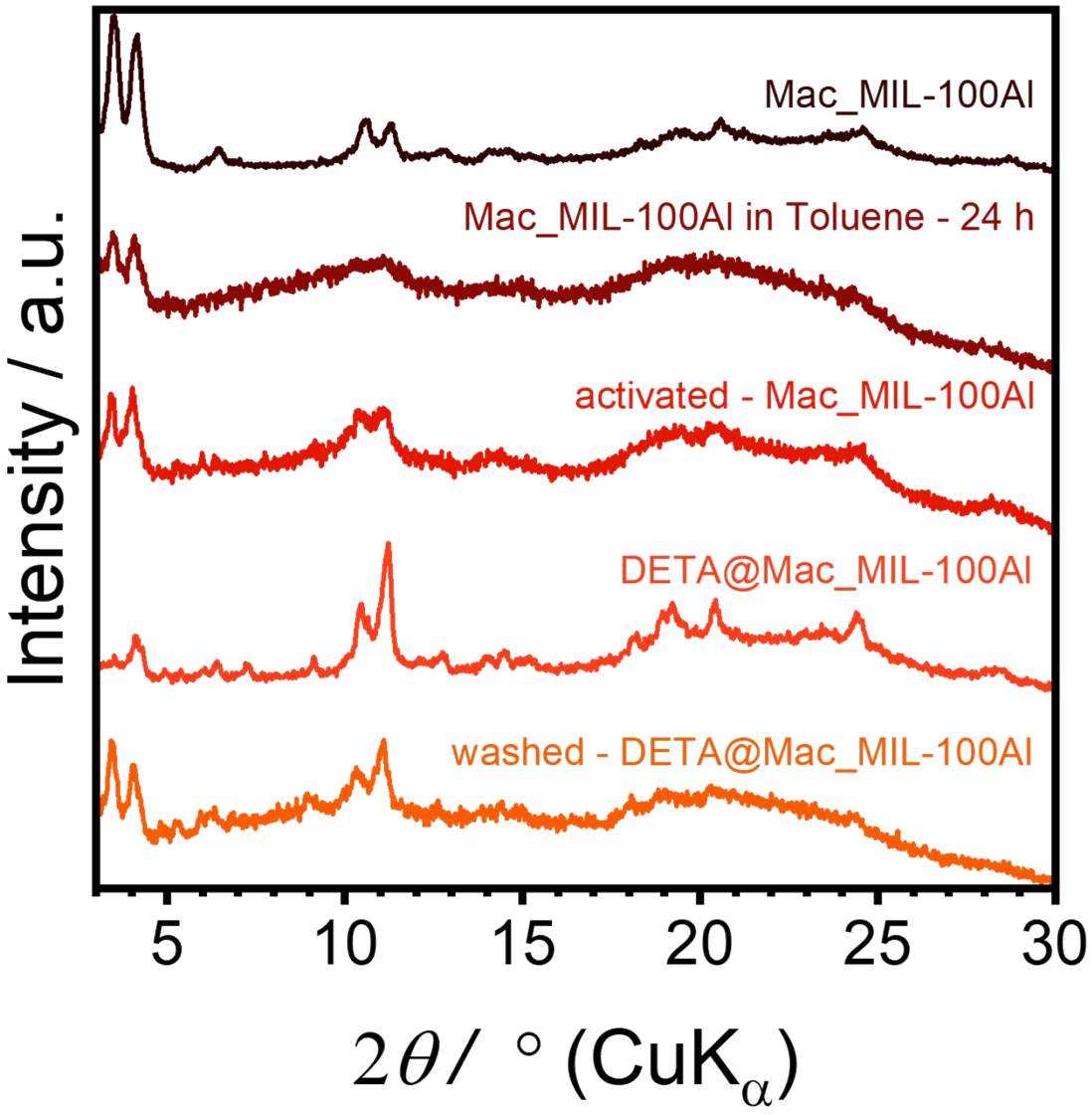

Figure S4. PXRD patterns of pristine Mac_MIL-100Al, Mac_MIL-100Al immersed in toluene for 24 h, toluene-treated Mac_MIL-100Al then activating at 150 °C under vacuum overnight, DETA@Mac_MIL-100Al, and MeOH-washed/activated DETA@Mac_MIL-100Al. The attenuation of low-angle reflections after solvent treatment and DETA incorporation indicates the sensitivity of MIL-100(Al) diffraction contrast to guest/solvent occupation and local structural disorder. The partial recovery of low-angle reflections after MeOH washing and activation suggests that the MIL-100(Al) framework is not completely collapsed and that part of the attenuation arises from removable or weakly adsorbed guest/amine species.

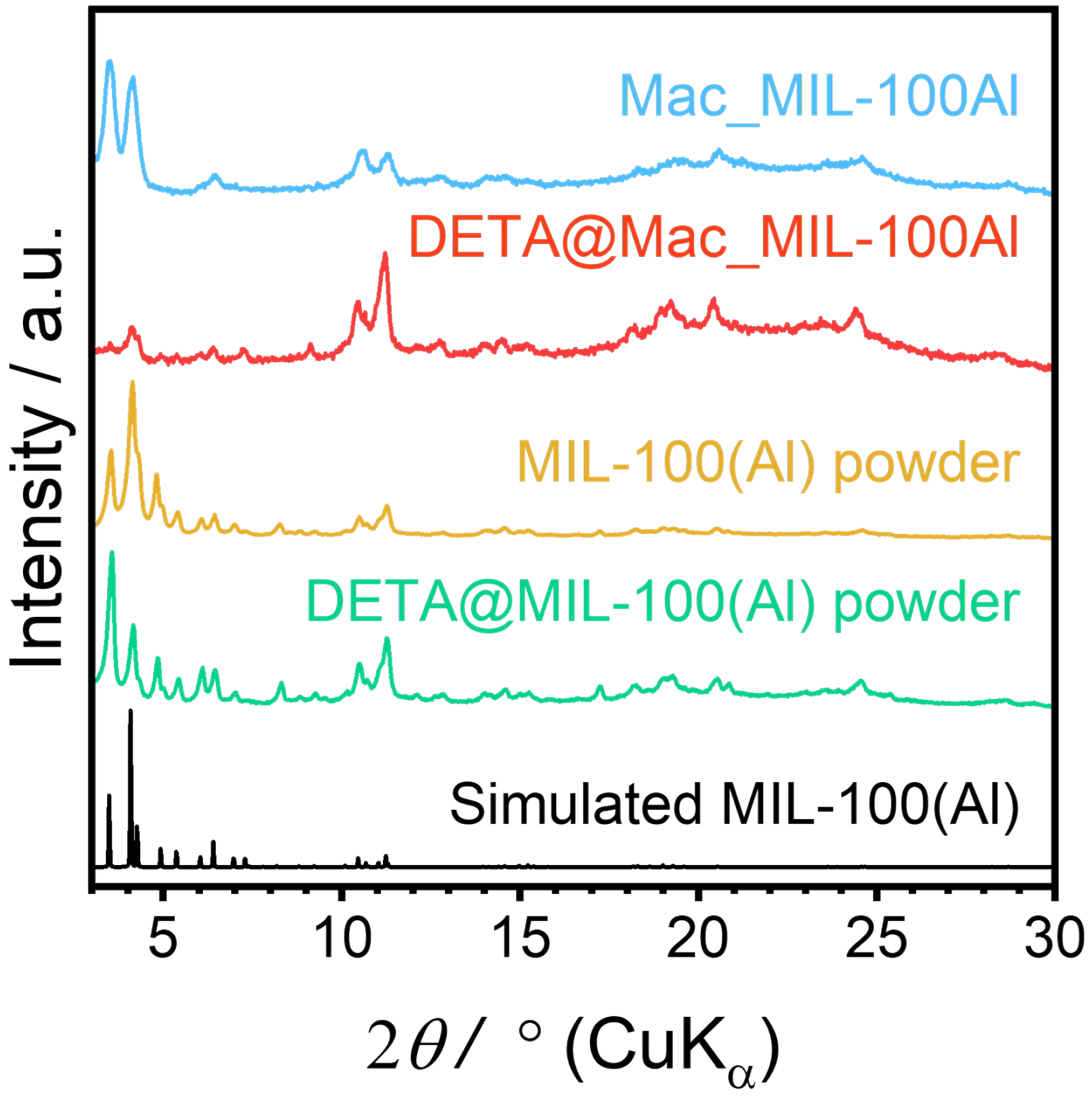

Figure S5. PXRD patterns of Mac_MIL-100Al, DETA@Mac_MIL-100Al, MIL-100(Al) powder, and DETA@MIL-100(Al) powder compared with the simulated MIL-100(Al) pattern.

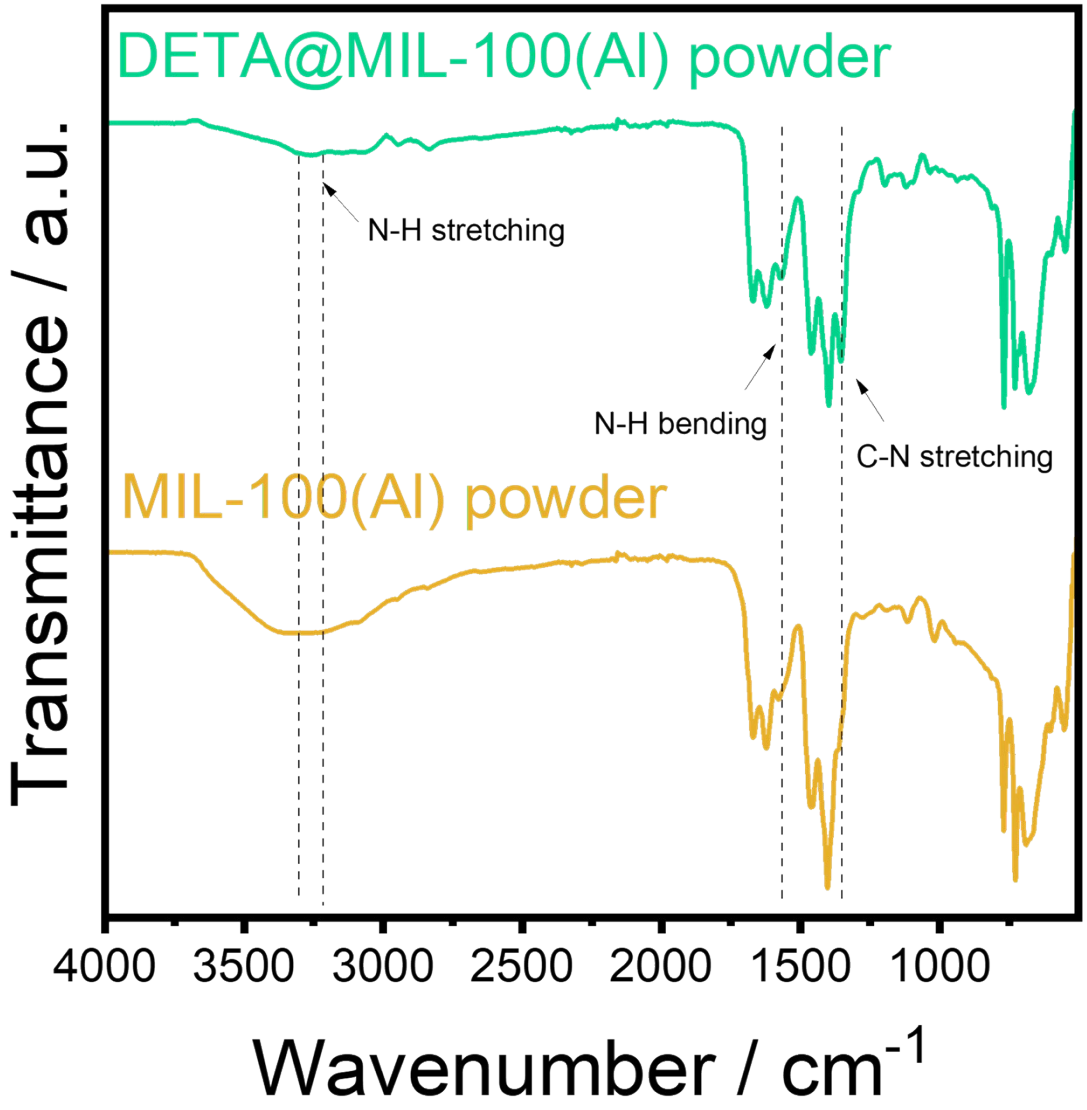

Figure S6. FTIR spectra of MIL-100(Al) powder and DETA@MIL-100(Al) powder. The appearance of N–H stretching/bending and C–N stretching bands after DETA treatment confirms amine incorporation, while the retained carboxylate vibrations indicate preservation of the MIL-100(Al) framework environment.

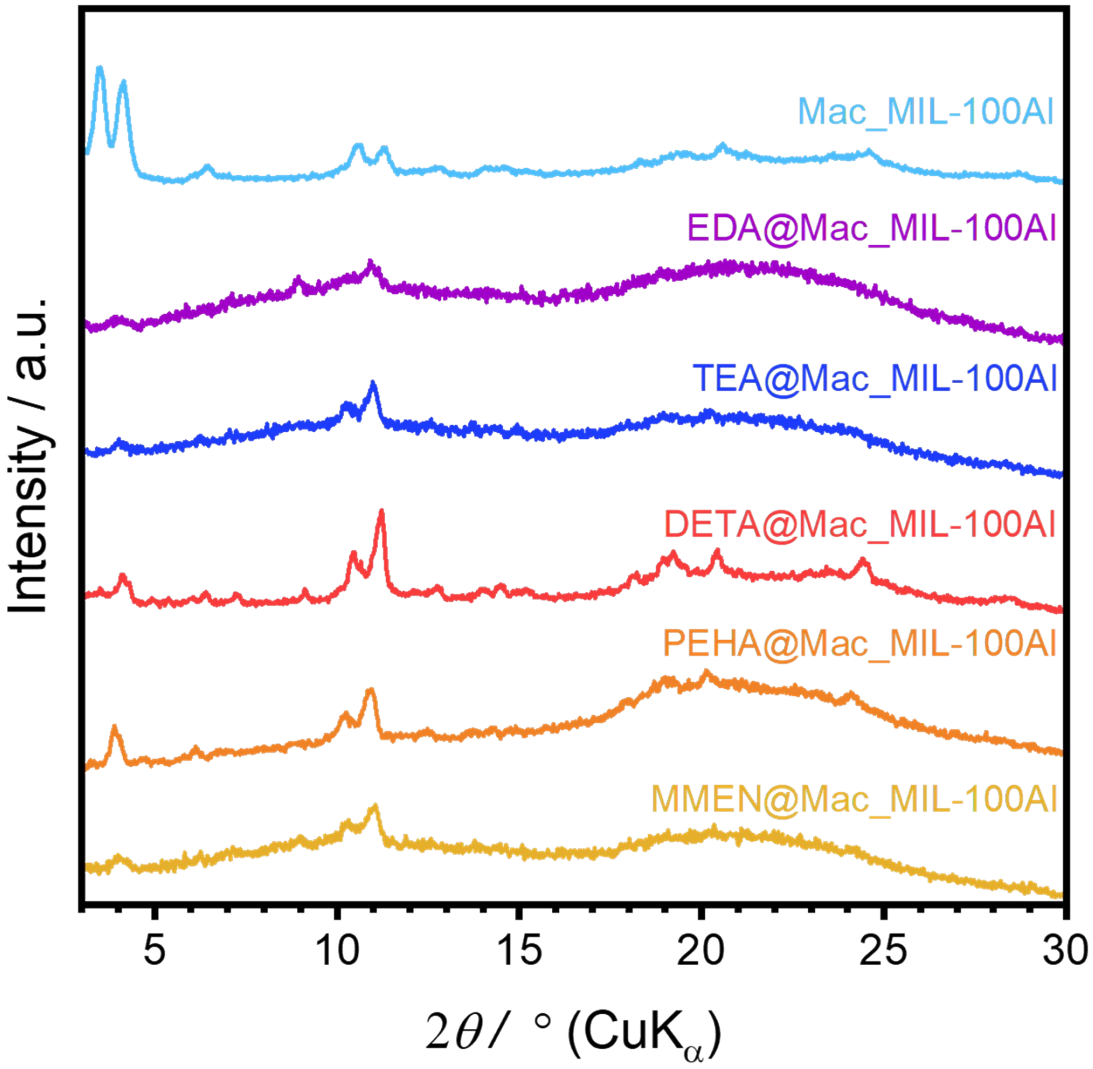

Figure S7. PXRD patterns of Mac_MIL-100Al beads functionalized with different amines: EDA – ethylenediamine, TEA – triethylamine, DETA – diethylenetriamine, PEHA – pentaethylenehexamine, MMEN – N, N'-dimethylethylenediamine.

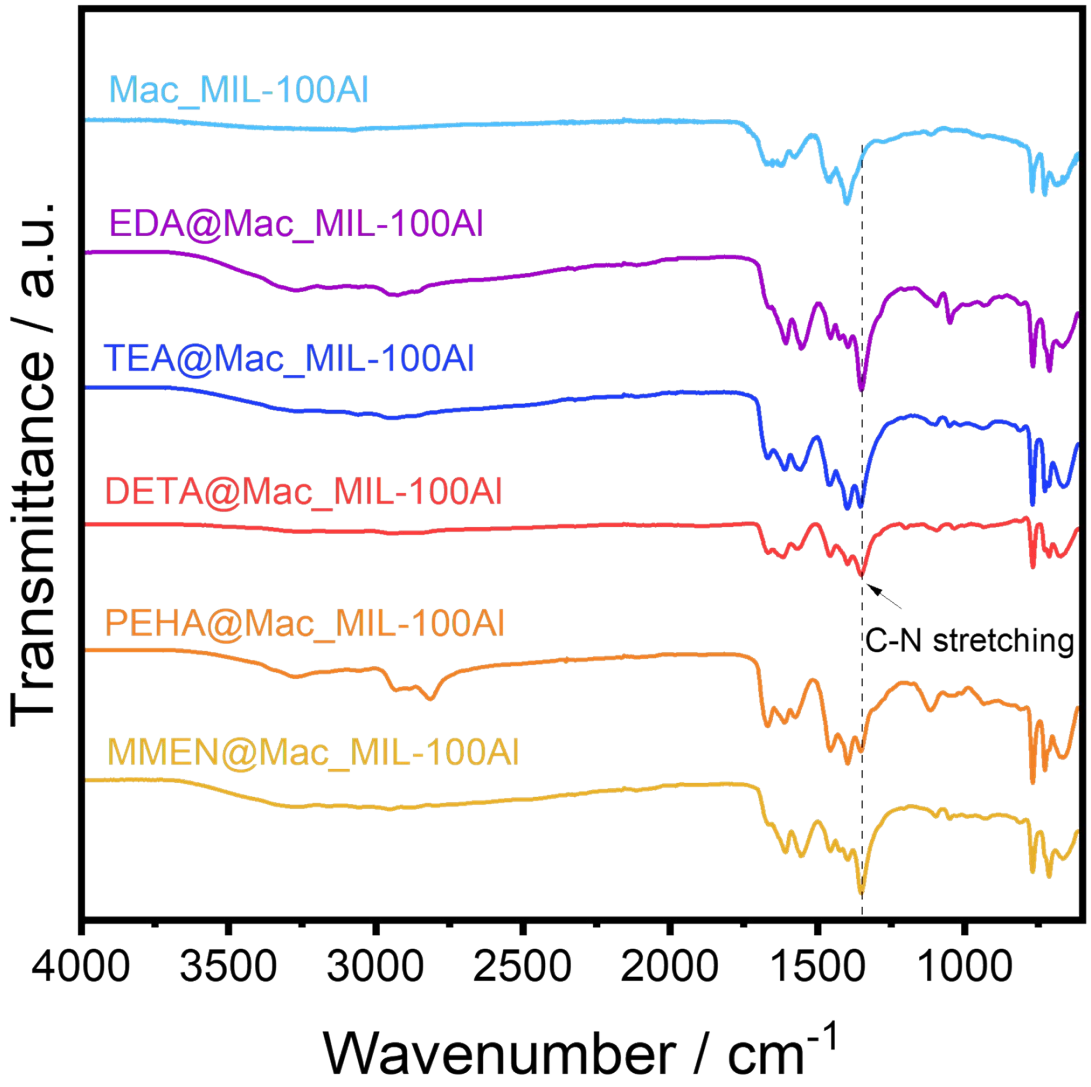

Figure S8. FTIR spectra of Mac_MIL-100Al beads functionalized with different amines: EDA – ethylenediamine, TEA – triethylamine, DETA – diethylenetriamine, PEHA – pentaethylenehexamine, MMEN – N, N'-dimethylethylenediamine.

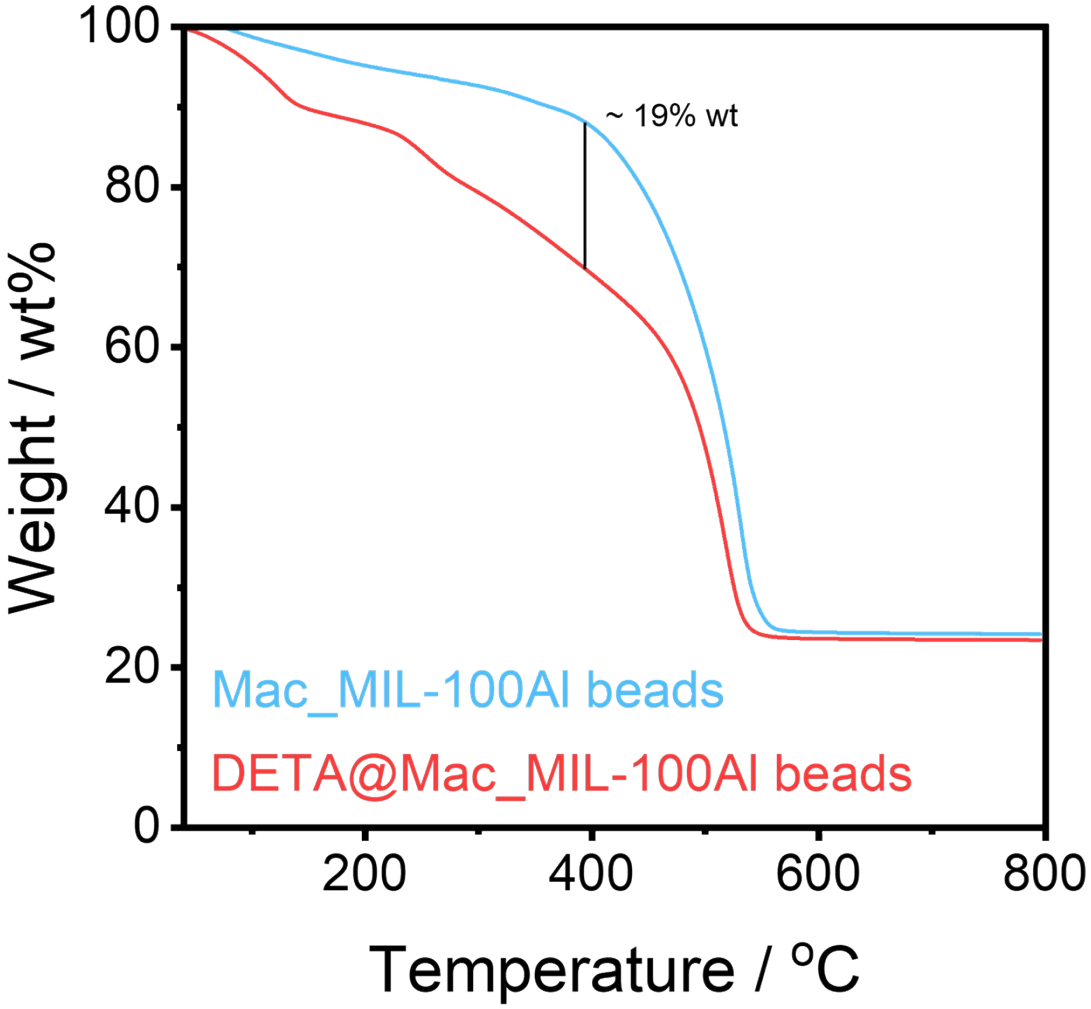

Figure S9. TGA curves of pristine Mac_MIL-100Al beads and DETA@Mac_MIL-100Al beads measured under air flow at a heating rate of 5 °C min^{-1}. The additional low-to-intermediate temperature mass loss observed for DETA@Mac_MIL-100Al is attributed to residual guest/solvent removal and decomposition/oxidation of incorporated DETA species, supporting successful amine incorporation. The high-temperature mass loss corresponds mainly to decomposition of the MIL-100(Al) framework.

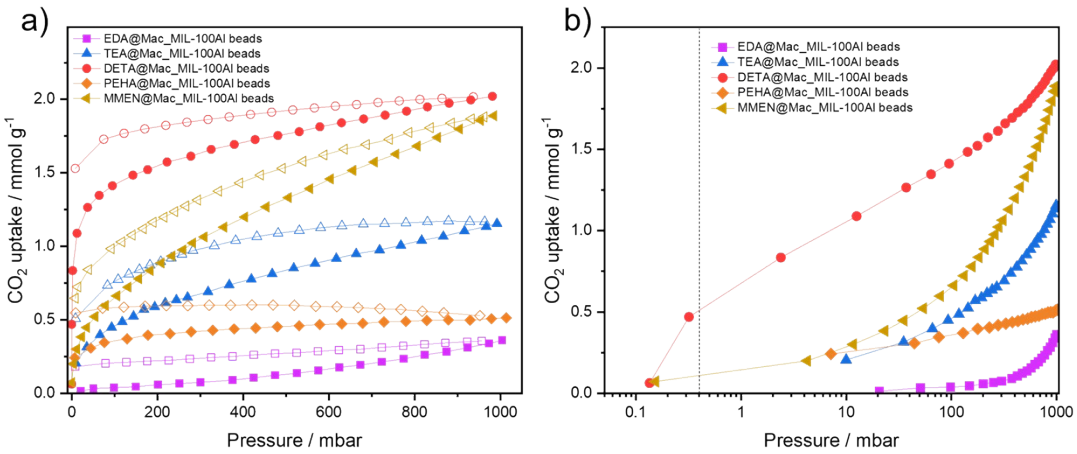

Figure S10. CO_2 adsorption isotherms measured at 298 K for DETA@Mac_MIL-100Al beads (red) (a) in comparison with different amines@Mac_MIL-100Al beads with pressure plotted on a linear scale; and (b) plotted on logarithmic scale (EDA-purple; TEA-dark blue; DETA-red; PEHA-orange; MMEN-brown).

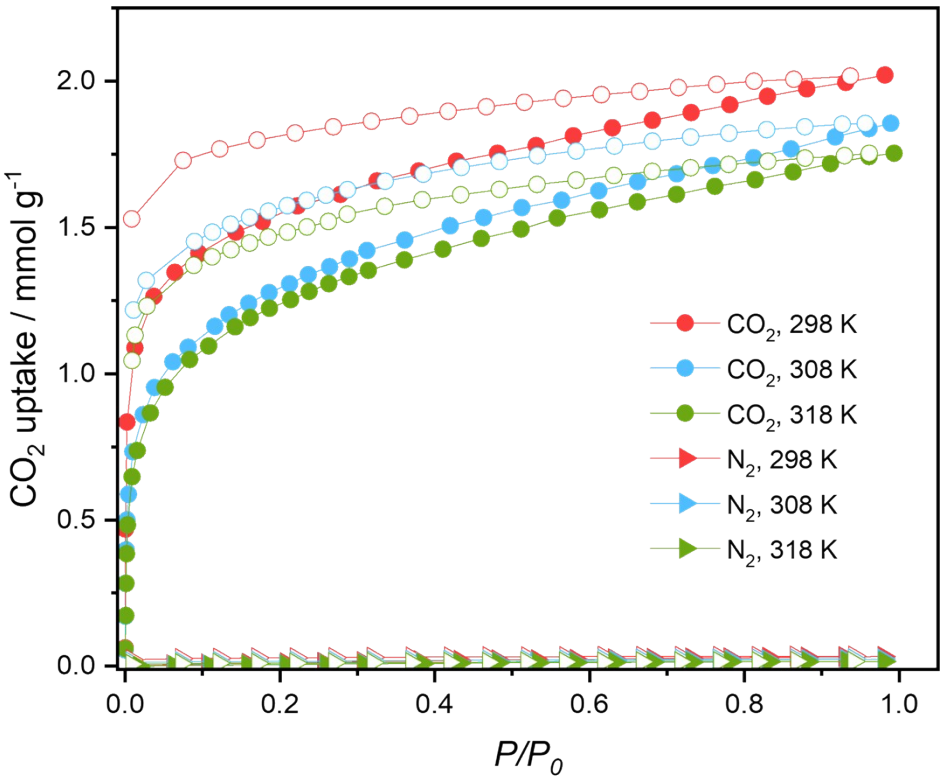

Figure S11. CO_2 and N_2 adsorption-desorption isotherms of DETA@Mac_MIL-100Al beads at 298 K – 308 K – 318 K.

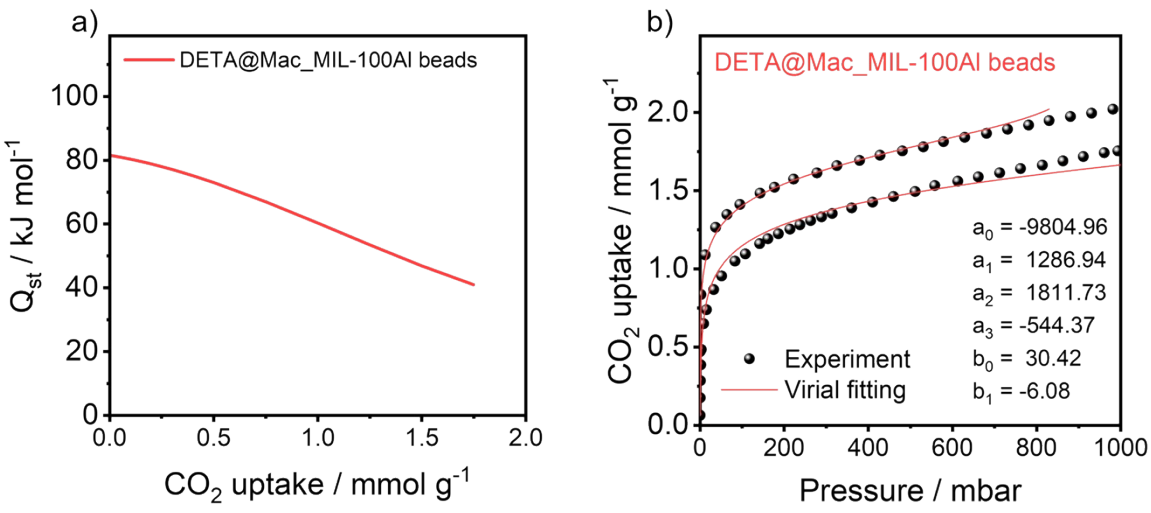

Figure S12. Isosteric heat of CO_2 adsorption (Q_{st}) (a) for DETA@Mac_MIL-100Al beads calculated using the virial fitting method (b). The Q_{st} decreases from approximately 81 kJ mol^{-1} at near-zero loading to approximately 40 kJ mol^{-1} at ca. 1.75 mmol g^{-1}.

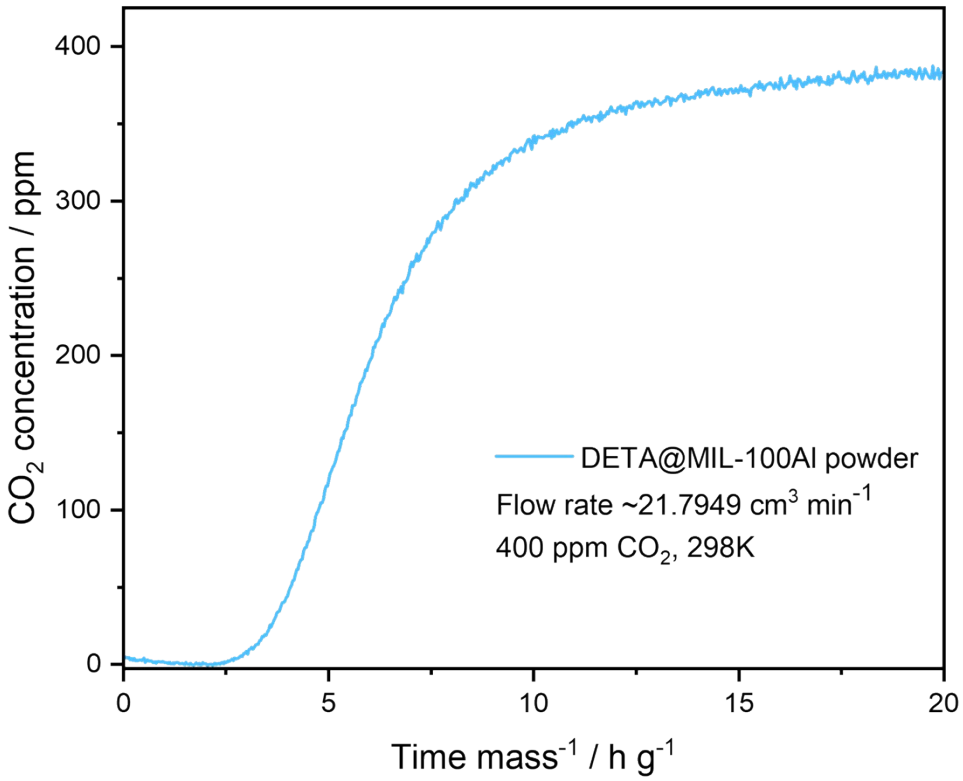

Figure S13. CO_2 breakthrough profile of DETA@MIL-100Al powder at the flow rate of 21.7949 ml min^{-1} for 400 ppm CO_2, 298 K.

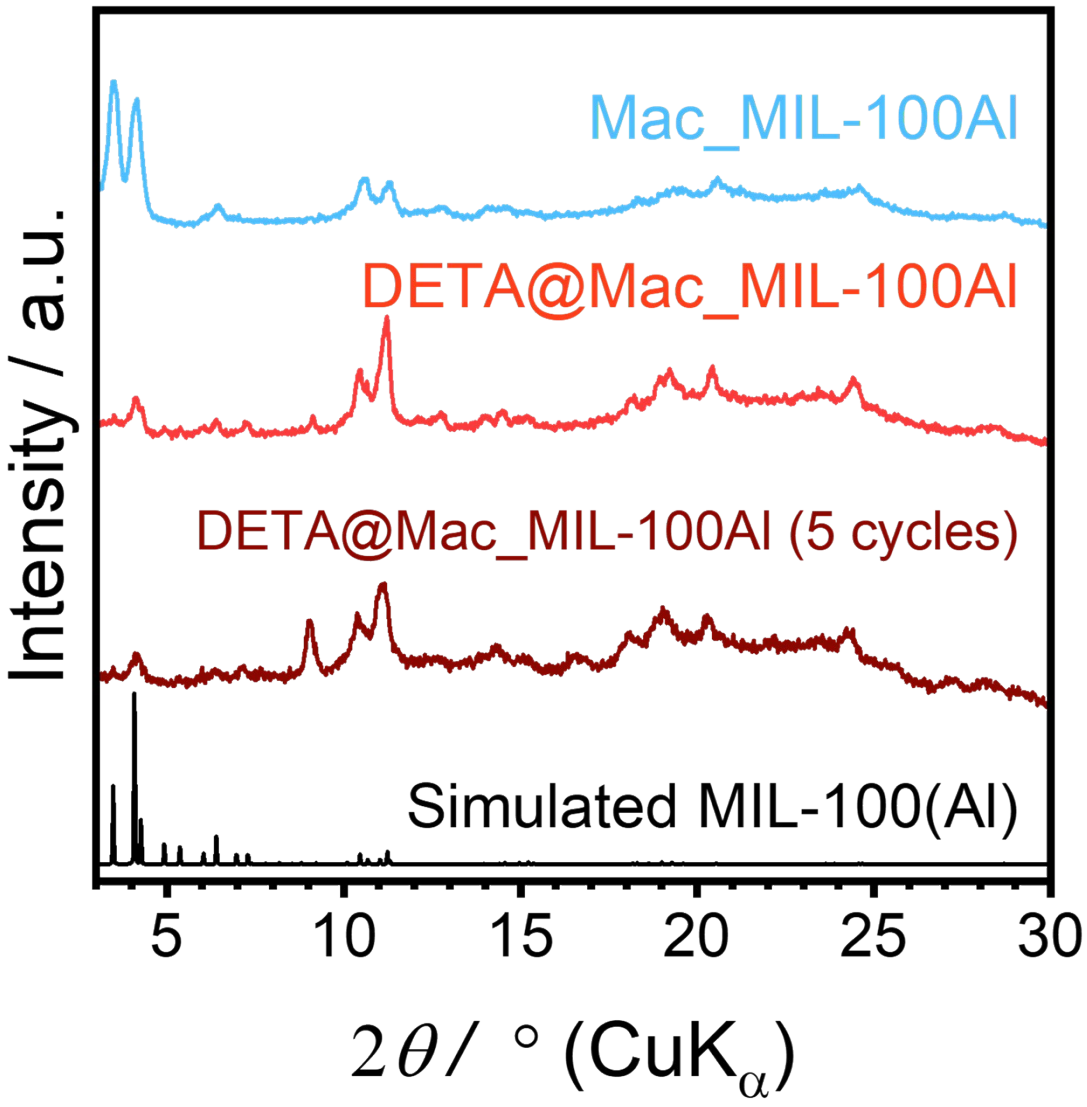

Figure S14. PXRD patterns of Mac_MIL-100Al, DETA@Mac_MIL-100Al, and DETA@Mac_MIL-100Al after five CO_2 adsorption–desorption cycles. The weak peak near $2\theta \approx 9°$ after cycling is tentatively assigned to a MIL-96(Al)-related reflection, indicating minor local rearrangement rather than extensive framework decomposition.

Section S3. Breakthrough Experiments

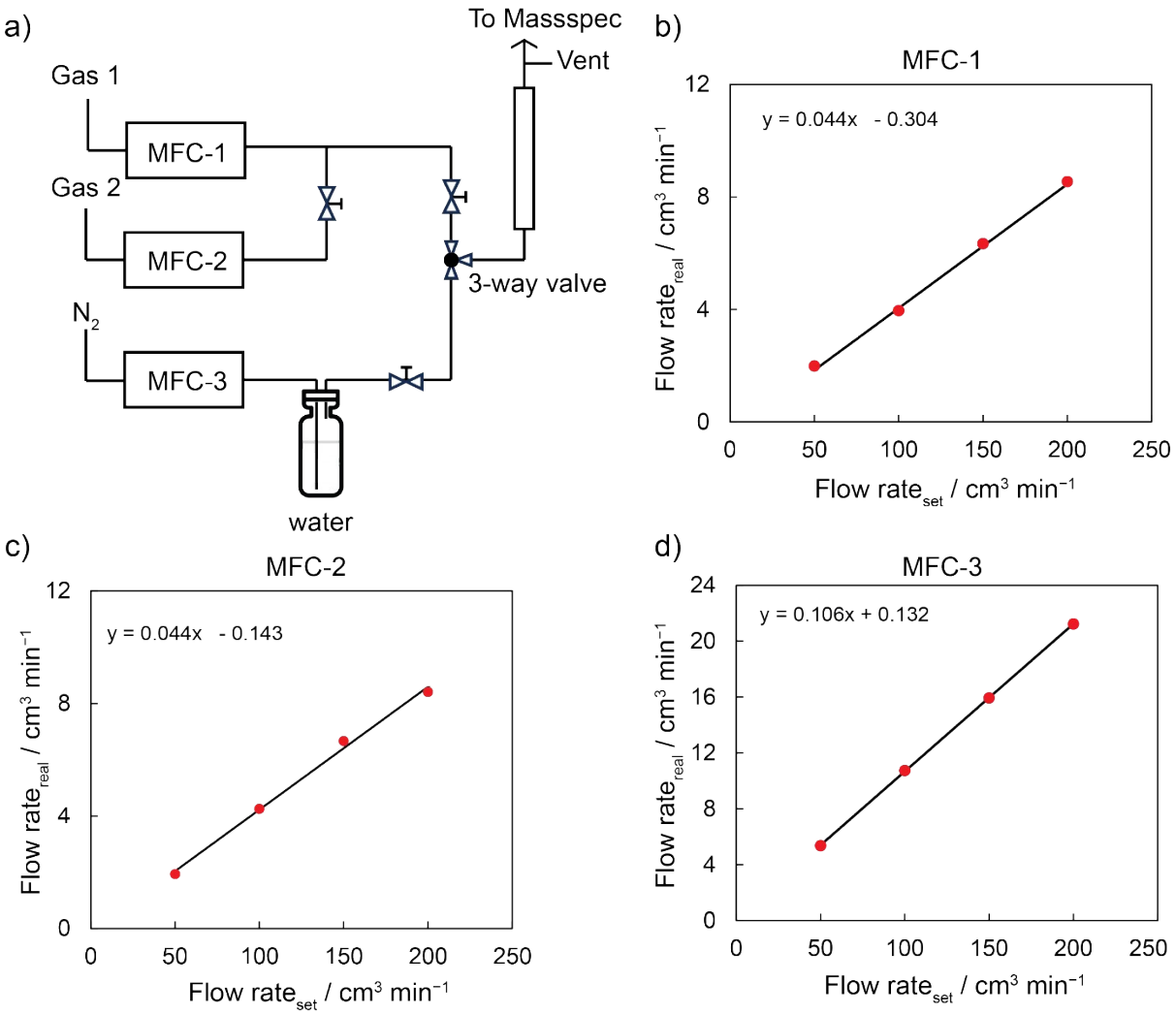

Figure S15. Customized system for analysis of the dynamic breakthrough adsorption: (a) the system diagram; and (b, c, d) the flow rate calibrations for MFC-1, 2 and 3.

Table S3. Comparison of DETA@Mac_MIL-100Al beads with representative shaped or structured adsorbents reported for DAC-relevant CO_2 capture. The table summarizes material form, CO_2 concentration, adsorption temperature, measurement method, and reported CO_2 uptake.

Adsorbents	Shape	CO_2 capture capacity @400ppm / mmol g^{-1}	Adsorption method	Refs
DETA@Mac_MIL-100Al beads	Beads ~2-3 mm	0.56	Breakthrough	This work
DETA@MIL-100Al powder	Powder	0.08	Breakthrough	This work
TRI-γ-Al_2O_3[(a)]	Pellet 3 mm	0.46	Breakthrough	[2]
Wash-coat TRI-γ-Al_2O_3[(a)]	Honeycomb monolith 2 x 2 x 0.4 mm	0.4	Breakthrough	[2]
Diamine-functionalized silica gel	Beads 2-5 mm	0.4	Temperature-concentration swing	[3]

Amine-Grafted SBA-15[(b)]	Pellet	0.09	Breakthrough	4
Li-LSX[(b)]	Pellet	0.82	Breakthrough	4
K-LSX[(b)]	Pellet	0.25	Breakthrough	4
NaX[(b)]	Pellet	0.32	Breakthrough	4
APS-SBA-15	Pellet 0.15-0.5 mm	0.53	CO_2 adsorption isotherm	5
A0.2P17	Monolith 3-4 mm	0.56	Breakthrough	6

(a) Measured at 430 ppm CO_2; (b) Measured at 395 ppm CO_2.

REFERENCES

1. T. N. Tu, P. N. Nguyen, H. T. Kwon and J. Kim, Chem. Eng. J., 2025, 519, 164997.
2. Q. Grossmann, V. Stampi-Bombelli, A. Yakimov, S. Docherty, C. Copéret and M. Mazzotti, Ind. Eng. Chem. Res., 2023, 62, 13594-13611.
3. J. A. Wurzbacher, C. Gebald and A. Steinfeld, Energy Environ. Sci., 2011, 4, 3584-3592.
4. A. N. Stuckert and R. T. Yang, Environ. Sci. Technol., 2011, 45, 10257-10264.
5. P. Bollini, N. A. Brunelli, S. A. Didas and C. W. Jones, Ind. Eng. Chem. Res., 2012, 51, 15153-15162.
6. P. Yuan, F. Huang, P. Li, H. Tian, Y. Zhou and T. Li, J. Environ. Chem. Eng., 2026, 14, 121233.